

# Invariant recognition of polychromatic images of *Vibrio cholerae* O1

**Josué Alvarez-Borrego**  
**Rosa Reyna Mouriño-Pérez**  
CICESE  
División de Física Aplicada  
Departamento de Óptica  
Km. 107 Carretera  
Tijuana-Ensenada  
Ensenada, B.C.  
México C.P. 22860  
E-mail: josue@cicese.mx

**Gabriel Cristóbal-Pérez**  
Instituto de Óptica (CSIC)  
Imaging and Vision Department  
Serrano 121  
E-28006 Madrid, Spain

**José Luis Pech-Pacheco**  
CICESE  
División de Física Aplicada  
Departamento de Óptica  
Km. 107 Carretera  
Tijuana-Ensenada  
Ensenada, B.C.  
México C.P. 22860  
and  
Instituto de Óptica (CSIC)  
Imaging and Vision Department  
Serrano 121  
E-28006 Madrid, Spain

**Abstract.** Cholera is an acute intestinal infectious disease. It has claimed many lives throughout history, and it continues to be a global health threat. Cholera is considered one of the most important emergence diseases due its relation with global climate changes. Automated methods such as optical systems represent a new trend to make more accurate measurements of the presence and quantity of this microorganism in its natural environment. Automatic systems eliminate observer bias and reduce the analysis time. We evaluate the utility of coherent optical systems with invariant correlation for the recognition of *Vibrio cholerae* O1. Images of scenes are recorded with a CCD camera and decomposed in three RGB channels. A numeric simulation is developed to identify the bacteria in the different samples through an invariant correlation technique. There is no variation when we repeat the correlation and the variation between images correlation is minimum. The position-, scale-, and rotation-invariant recognition is made with a scale transform through the Mellin transform. The algorithm to recognize *Vibrio cholerae* O1 is the presence of correlation peaks in the green channel output and their absence in red and blue channels. The discrimination criterion is the presence of correlation peaks in red, green, and blue channels.  
© 2002 Society of Photo-Optical Instrumentation Engineers. [DOI: 10.1117/1.1456539]

Subject terms: scale transform; *Vibrio cholerae* O1; image processing; correlation function.

Paper 010034 received Feb. 5, 2001; revised manuscript received Oct. 5, 2001; accepted for publication Nov. 16, 2001.

## 1 Introduction

In the 1980s the estuarine origin of *Vibrio cholerae* O1 and its link with marine organisms was documented. There are many questions about the ecology of the cholera bacteria that remain unsolved. Better knowledge of the cholera bacteria's behavior in ocean and coastal zones could lead to accurate predictions of cholera outbreaks and slowing the spread of cholera pandemics. In this case, the long-term environmental monitoring of *Vibrio cholerae* O1 in seawater could be the answer to many open questions concerning cholera. Different human-driven techniques to recognize the bacteria have experienced some reliability difficulties.

The performance of ecological studies of microscopic organisms greatly depends on the correct identification and quantification of the organism under study in natural environments. For instance, *Vibrio cholerae* O1 is responsible for cholera disease and there are many unsolved questions about its ecology that could be answered through the observation of a large number of seawater samples worldwide.<sup>1,2</sup>

Microbiologists have developed several techniques for bacteria identification. *Vibrio cholerae* O1 has usually been

identified through cultures in specific media and a waterfall of biochemical tests.<sup>3</sup> Nevertheless, *Vibrio cholerae* could survive in an adverse environment in a dormancy stage. This stage has been called "viable but not culturable," and bacteria cannot be recovered by culture methods.<sup>4,5</sup> On the other hand, to develop all these tests we require at least 5 days, and it is finally necessary to use direct methods.<sup>6</sup>

Molecular biology techniques such as protein chain reaction are the most specific methods of bacteria typing. They determine the protein composition of the bacteria wall and deoxyribonucleic acid, but they are expensive, sophisticated, and complicated tools and we may not use them for screening proposal.<sup>7</sup>

Direct techniques such as staining with acridine orange and DAPI have also been used, but these methods are inaccurate methods that provide information about presence only of organic matter or organisms in general.<sup>8,9</sup> Direct fluorescent antibodies (DFA) is a fast and highly specific staining method;<sup>10-12</sup> however, the samples processed with DFA should be evaluated by an experienced observer, whose capacity depends on the sample number. Slide reading is a boring activity that consumes a lot of time, produce

tiredness, and decreases the observation reliability when the number of samples increases.

The different human-driven techniques to recognize bacteria have some reliability difficulties. Automated methods such as optical systems represent a new possibility to make better measurements of the presence and quantity of this microorganism in its natural environment. Automatic systems eliminate observer bias, reduce analysis time, relieve researchers of the tedious activity of organism identification and counting, and provide major effectiveness.

Optical systems are becoming an interesting tool for biologists to make easier and better observations of the presence of microorganisms in an environment. Since VanderLugt introduced the filtering techniques,<sup>13</sup> optical correlation methods based on object shape have been successfully used in pattern recognition. Several kinds of filters have been developed to recognize different objects. In biology, for example, we have the use of circular harmonic filters for copepods recognition<sup>14</sup> and matched filtering to determine for different phytoplankton species.<sup>15</sup>

Nevertheless, the recognition of particular bacteria species is a complex issue. Bacteria shape does not provide enough information to identify them, because there are many species that share the same shape. *Vibrio cholerae* O1 has a transparent curved rod shape, the same as all members of the Vibrionaceae family among others.<sup>3</sup> To solve this problem, we can mark *Vibrio cholerae* O1 with monoclonal antibodies, giving them a specific green color,<sup>12</sup> and use optical color correlation systems to increase the discrimination ability of pattern recognition filters, taking into account only color and shape information.<sup>16–19</sup> Bacteria color and shape depends on the illuminating wavelength; that is, color introduces additional information to improve recognition effectiveness. The logical or arithmetic sum of polychromatic object decomposition in three simple monochromatic channels [red, green, and blue (RGB)] produces a high level of target recognition.

Bacteria's morphology, orientation, and size changes are other problems that we must tackle. Besides shape and color, our optical system must be invariant to position, scale, and rotation. We use the digital scale transform through the Mellin transform approach<sup>15</sup> to implement an optimal process that guarantees a high discrimination capability of invariant pattern recognition correlators. To our knowledge, this approach has never been used in color systems. Our goal is to evaluate the effectiveness of color correlation systems for *Vibrio cholerae* O1 recognition, and also develop invariant filters by comparing the performance of matched filters with phase-only filters.

Section 2 presents a summary of the importance of the cholera study. Section 3 describes the *Vibrio cholerae* O1 samples, Sec. 4 describes the invariant recognition system for cholera identification. Finally, Sec. 5 presents some results and discussion.

## 2 Cholera Importance

Cholera has claimed many lives throughout history, and it continues to be a global health threat. Since the first documented modern pandemic in 1817, six more pandemics have occurred.<sup>20–22</sup> The origin of these cholera pandemics is mysterious. One hypothesis holds that *Vibrio cholerae*

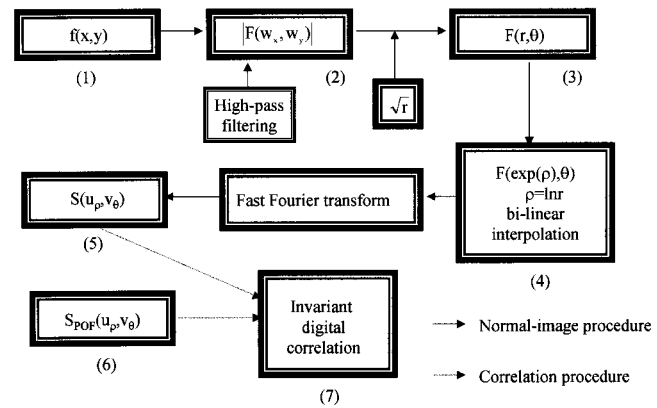


Fig. 1 Steps of scale transform via the Mellin transform.

O1 exists in a nonpathogenic state, and local environmental changes, perhaps related to the season, promote its shift to virulence.<sup>4,22</sup>

In support of this hypothesis there is recent evidence that the cholera bacillus can survive indefinitely in some hostile natural environments.<sup>4,11,23–26</sup> The starting points for nearly all cholera epidemics appear to be port communities, implying a role for a marine transmission. We must consider more carefully the possible role of the ocean in the spread of the cholera bacillus worldwide.

The biogeography of the ocean changes with the seasons, in a fashion analogous to changes on land. Most ocean cycles result from dynamic displacement of transitional, highly compressed gradients in the atmospheric and subsequent oceanic interactions.<sup>27,28</sup> Ecological studies have documented seasonal, annual, decadal, and longer term responses to climate-driven environmental changes. Changes in species distribution and prevalence, for bacteria as well as larger organisms, also reflect climate-driven ocean variation.<sup>27,29</sup> In this case, the long-term environmental monitoring of *Vibrio cholerae* in seawater could be the answer to many questions about the cholera.

## 3 *Vibrio cholerae* O1 Samples

*Vibrio cholerae* O1 Inaba E1 Tor was used to inoculate one flask with 160 ml of seawater simulated with 20% salinity, enriched with 0.5% peptone, and incubated at 25°C. Samples of 10  $\mu$ l were processed with the DFA 10 to 12 technique to stain *Vibrio cholerae* O1 cells and observed under a Carl Zeiss epifluorescence microscope. Images from the bacteria found in the laboratory samples were recorded with a CCD color camera. These images,  $f(x)$ , were used for the automated invariant recognition of *Vibrio cholerae* O1 with the system described here. The monoclonal antibodies technique is an accurate procedure to mark *Vibrio cholerae* O1 with almost 100% of sensitivity.<sup>10–12</sup>

## 4 Invariant Color Object Recognition

A numerical simulation was performed to correlate *Vibrio cholerae* O1 with phase-only filters (POFs). Figure 1 shows seven steps for invariant correlation of rotation, scale, and position. All steps were developed digitally. The 1-D scale transform is given by

$$S(u_x) = \frac{1}{\sqrt{2\pi}} \int_0^\infty f(x) \frac{\exp(-ju_x \ln x)}{\sqrt{x}} dx, \quad (1)$$

where  $u_x$  is the new coordinate of the image. Because the main operation realized by the lens in an optical system is the Fourier transform,<sup>30</sup> and because it is digitally easier to use the fast Fourier transform (FFT), we show that we can compute the scale transform through the Fourier transform (whose magnitude is position invariant). This is feasible, since any linear mathematical operation, can be written in the general form

$$g(\alpha) = \int_{x_1}^{x_2} f(x) K(\alpha, x) dx, \quad (2)$$

where  $g(\alpha)$  is<sup>31</sup> the integration of the product of the function  $f(x)$  with the kernel  $K(\alpha, x)$ , and  $\alpha$  is any variable. The only difference between the two transforms is thus the kernel  $K(\alpha, x)$ .

Let us consider the Fourier transform of a function  $f(x)$ :

$$g(\alpha) = \int_{x_1}^{x_2} f(x) \exp(-j\alpha x) dx, \quad (3)$$

where  $\exp(-j\alpha x)$  is the Fourier kernel transformation. The Mellin transform can be written as

$$g(\alpha) = \int_{x_1}^{x_2} f(x) x^{j\alpha-1} dx, \quad (4)$$

where  $x^{j\alpha-1}$  is the Mellin kernel transformation, and  $x_1$  and  $x_2$  are the limits in the integral. Thus, it is possible to proceed from the scale to the Fourier transform via Mellin transform. In this section, we write the relation between the scale and the Mellin transform only. This is important because, in this way, Eq. (1) can be manipulated via Fourier transform throughout the Mellin transform easily.

The separable 2-D scale transform  $S(u_x, v_y)$  is used in this correlation process because it is invariant to size changes. Its definition is given by<sup>32</sup>

$$S(u_x, v_y) = \frac{1}{\sqrt{2\pi}} \int_0^\infty \int_0^\infty f(x, y) \frac{\exp(-ju_x \ln x - jv_y \ln y)}{\sqrt{xy}} dx dy, \quad (5)$$

where  $(u_x, v_y)$  represent the scale variables. It is easy to show that the scale transform of the function  $g(x, y) = [f(x, y)]/\sqrt{xy}$  is given by

$$S(u_x, v_y) = F\{f[\exp(p), \exp(q)]\}, \quad (6)$$

where  $F$  is Fourier transform.

Thus, relations between the scale with Mellin transforms in two dimensions, in one as in another sense, are<sup>33</sup>

$$\begin{aligned} \text{scale transform} \left[ g(x, y) = \frac{f(x, y)}{\sqrt{xy}} \right] \\ \equiv \text{Mellin transform}[f(x, y)], \end{aligned} \quad (7)$$

$$\text{Mellin transform}[\sqrt{xy}f(x; y)] \equiv \text{scale transform}[f(x, y)]. \quad (8)$$

Thus, via the Mellin transform we can calculate the scale transform or vice versa. According to Eq. (8), between steps 2 and 3 we introduce the factor  $\sqrt{r}$  (Fig. 1), and in this way, we obtain the scale transform via the Mellin transform. The effect of this factor on the module of FFT is radial only.

According to Casasent and Psaltis,<sup>34</sup> it is easier to calculate an invariant correlation to scale by performing a warping of the input function and subsequently a Fourier transform (Fig. 1). Initially in step 1 (Fig. 1), we have an input function  $f(x, y)$  for which a calculation of the module of the FFT  $|F(w_x, w_y)|$  (step 2) is made; this avoids any shift of the input function  $f(x, y)$ . When input function  $f(x, y)$  rotates by a certain angle  $\theta$ ,  $|F(w_x, w_y)|$  rotates at the same angle, and a change in scale  $a$  in  $f(x, y)$  magnifies  $|F(w_x, w_y)|$  by  $|a|^{-1}$ .

The effects of change in rotation and scale can be separated by the polar transformation of  $|F(w_x, w_y)|$  from coordinate  $(w_x, w_y)$  to coordinate  $(r, \theta)$ . Because  $\theta = \tan^{-1}(w_y/w_x)$  and  $r = (w_x^2 + w_y^2)^{1/2}$ ,  $a$  changes the scale of  $|F(w_x, w_y)|$ , and the  $r$  coordinate becomes  $r' = ar$  without affecting the  $\theta$  coordinate. Thus, a change in scale of a bidimensional input function is a change in scale of only one dimension ( $r$  coordinate) in the function  $F(r, \theta)$  (step 3 in Fig. 1). To maintain not only the scale but the rotational invariance we use the nonseparable scale transform, by taking the log of the radial coordinate  $\lambda = \ln(x^2 + y^2)^{1/2}$

$$\begin{aligned} S(u_\rho, u_\theta) = \frac{1}{\sqrt{2\pi}} \int_0^\infty \int_0^{2\pi} f(\lambda, \theta) \exp(\lambda/2) \\ \times \exp(-j\lambda c_\rho - j\theta c_\theta) d\lambda d\theta. \end{aligned} \quad (9)$$

Now, this process is quite different from the process presented by Casasent and Psaltis<sup>34</sup> in two aspects: first, because the high frequencies present in the module of the FFT have important information of features of the original images we enhance high-pass filtering effect,<sup>35</sup> which consists of applying a parabolic function to the FFT module. In this way, low frequencies are attenuated and high frequencies are enhanced in proportion to  $w_x^2$  and  $w_y^2$ , and second, in step 4 (Fig. 1), a variable change is made with respect to  $r$ :  $F[\exp(\rho), \theta]$ , where  $\rho$  is  $\ln r$ , and in this transformation we encountered an aliasing problem. We applied a bilinear interpolation to avoid this effect.<sup>33</sup>

In step 5 (Fig. 1) we obtain the bidimensional scale transform via an FFT. POFs  $S_{\text{POF}}(u_\rho, v_\theta)$  are defined as

$$S_{\text{POF}}(u_\rho, v_\theta) = \exp[-i\phi(u_\rho, v_\theta)], \quad (10)$$

where  $|S(u_\rho, v_\theta)|$  is equal to one, and  $u_\rho$  and  $v_\theta$  are variables in the frequency domain (step 6). Correlation of the

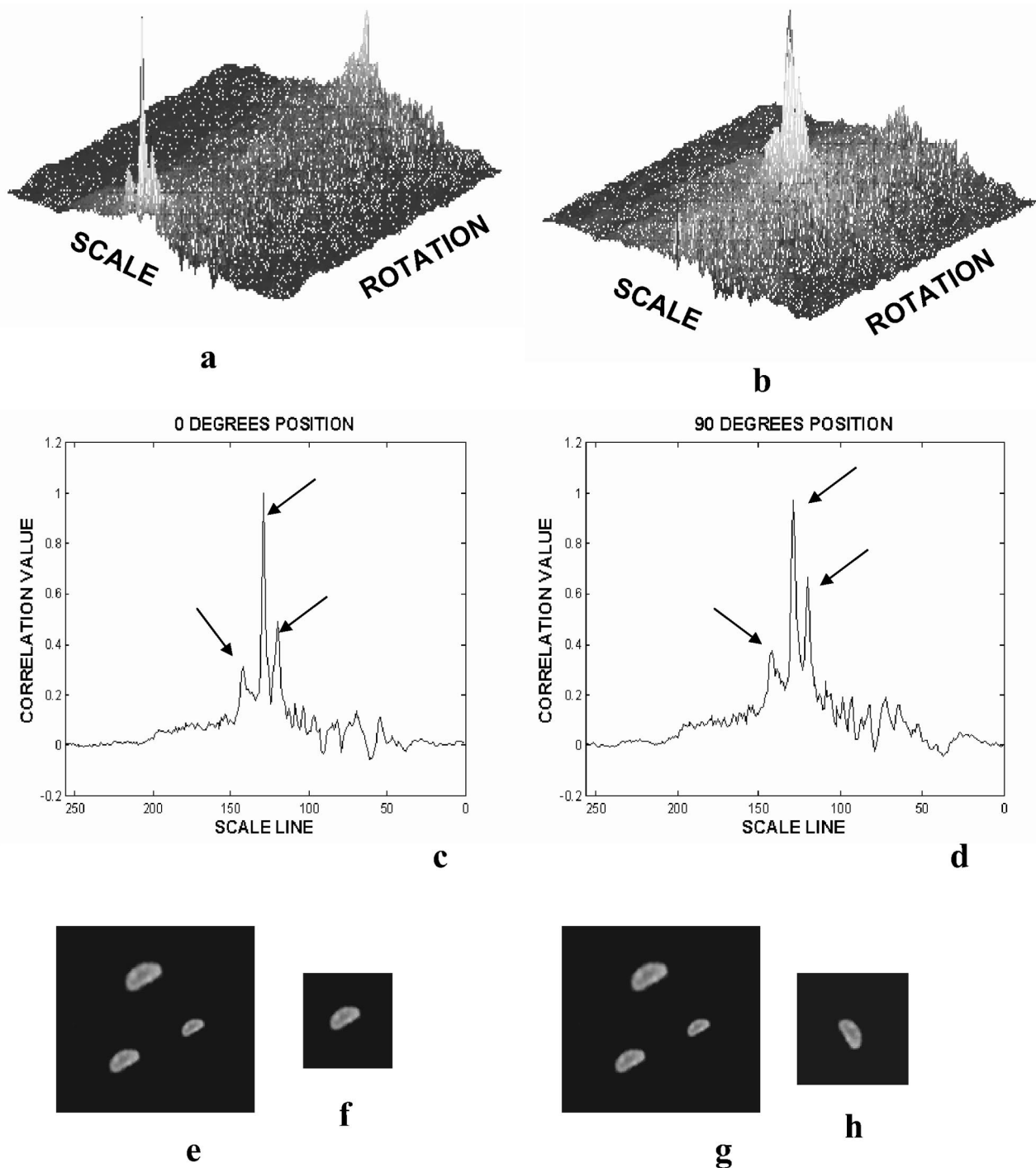


**Fig. 2** Correlation with scale transform: (a) and (b) correlation outputs in the green channel with POFs, (c) graph of a line 1 of (a), (d) graph of a line to 90 deg. of (b), (e) and (g) problematic images in the green channel, and (f) and (h) filter images in the green channel.

digital filter (step 7) with the scale transform of the image generates very low correlation values for geometrically dissimilar organisms and high correlation values for geometrically similar organisms.

As mentioned, the recognition of particular species of bacteria is a complex issue. Bacteria shape does not provide enough information to identify them, because there are many species that share the same shape. In the specific case of *Vibrio cholerae* O1, color information becomes an im-

portant discriminant feature that we must include in the whole identification process.

In general, a polychromatic object presents a different shape and amplitude distribution  $A_{\lambda_i}(x,y)$  when illuminated with different wavelength  $\lambda$ . However, two different objects may present similar amplitude distributions when they are illuminated with the determined wavelength  $\lambda_0$ . Thus, in an optical pattern recognition process using a cor-

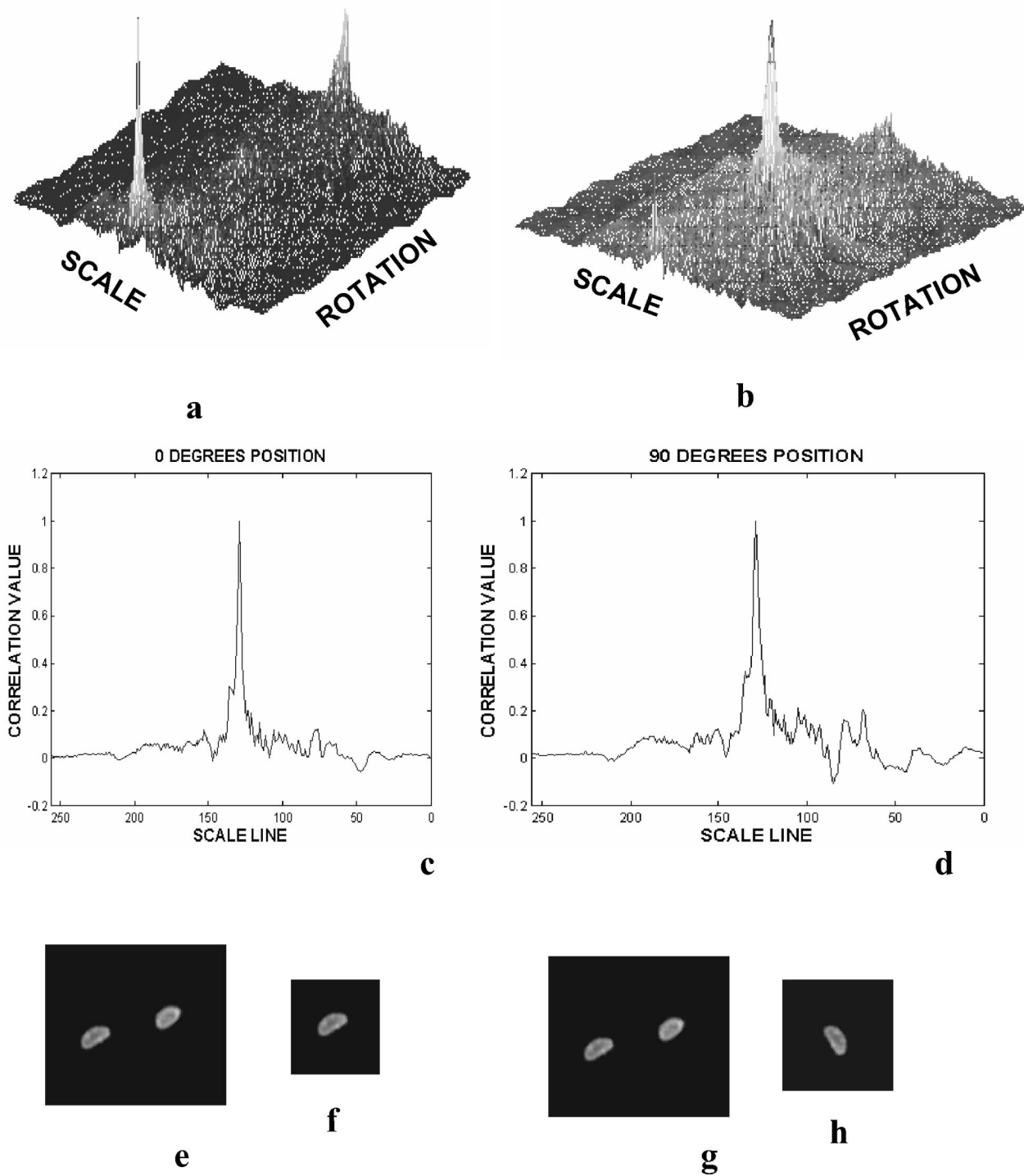


**Fig. 3** Correlation with scale transform: (a) and (b) correlation outputs in the green channel with POFs, (c) graph of a line at 0 deg of (a), (d) graph of a line at 90 deg of (b), (e) and (g) problematic images in the green channel, and (f) and (h) filter images in the green channel.

relator illuminated with a wavelength  $\lambda_0$ , these objects will give very similar amplitude correlation distributions, and some false alarms will appear. To avoid this problem, it is necessary to use the information about the dependence of the object amplitude distributions on wavelength.<sup>36</sup>

Most of the natural colors can be obtained as a combination of three colors (the so-called primary colors) if they are well selected. Each of them must be in the red (R),

green (G), and blue (B) regions of the visible spectrum, respectively. When the object is a transparency, the amplitude transmittances obtained with illumination of one of these primaries are called the red, green, and blue components of the object.

The recognition of an object in a scene is achieved by decomposing the information in three monochromatic channels and by identifying the object in each channel in-

dependently. In other words, the correlation  $C_{\lambda_i}(x,y)$  between the scene to be analyzed  $f_{\lambda_i}(x,y)$  and the bacteria to be detected  $B_{\lambda_i}(x,y)$ , in this case, are obtained by illuminating an optical setup with three wavelengths  $\lambda_i = R, G, B$ , which cover the visible spectrum:

$$C_{\lambda_i}(x,y) = f_{\lambda_i}(x,y) \otimes B_{\lambda_i}(x,y). \quad (11)$$

Thus, the process shown in Fig. 1 will be repeated for each channel ( $R$ ,  $G$ , and  $B$ ). In each channel, the filter to be used is matched to the corresponding component of the target. In general, objects that have a determined component  $A_{\lambda_i}(x,y)$  similar to component of the target  $B_{\lambda_i}(x,y)$  will give a maximum of correlation in this channel ( $\lambda_i$ ). But only the target will simultaneously give a correlation maximum in each channel. Thus, an object is detected as the target if it simultaneously produces a correlation peak in the three channels. In the particular case of *Vibrio cholerae* O1, however, we could mark it with a specific green color with monoclonal antibodies. Thus, the correct identification for these bacteria will be in the green channel only, and the presence of correlation peaks in the other two channels will constitute a false identification.

Therefore, with the methodology described, it is possible to recognize *Vibrio cholerae* O1 in a digital correlator invariant to rotation, position, and scale changes.

## 5 Results and Discussion

Some examples of invariant correlation outputs in the green channel of *Vibrio cholerae* O1, using the methodology shown in Fig. 1, are shown in Figs. 2 and 3. Figure 2(e) shows an image with three bacterias with the same angle but for three different sizes (120, 100, and 60%) with respect to the filter [Fig. 2(f)]. The output in the green channel shows three peaks at 0 deg [Fig. 2(a)]. A profile of these peaks are shown in Fig. 2(c). The one in the middle corresponds to 100%, the one beside it to the left to 60%, and the one beside it to the right to 120%. Other peaks at 180 deg are present because of the periodicity produced by the polar transform. In the output, there is a change in the position of the correlation peak corresponding to the size and angle differences with the filtered organism.

Invariant correlation results in the green channel with a filter that has an organism of different orientation (90 deg) [Fig. 2(h)] are shown [Fig. 2(b)]. Three correlation peaks are present at 90 deg, which is the angle of bacteria in image [Fig. 2(g)] with respect to bacteria in the filter. A profile of the line at 90 deg shows three correlation peaks [Fig. 2(d)]. The left arrow represents larger bacteria, the arrow in the center, the middle organisms, and the right arrow, the smallest bacteria.

Figures 3(e) and 3(g) present two organisms with minimal scale and rotation differences. This image was correlated with a filter with the same orientation and similar size [Fig. 3(f)]. We observe a unique correlation peak at 0 deg and its harmonic at 180 deg [Fig. 3(a)]. A profile of this result is shown in Fig. 3(c). Even though there are two bacteria in the image test, there is just one peak in the output because when the organisms are similar in size and orientation the peaks are superimposed. This constitutes a

trade-off for organism count, but this invariant process improves the recognition efficiency because the correlation is invariant to position, scale, and rotation.

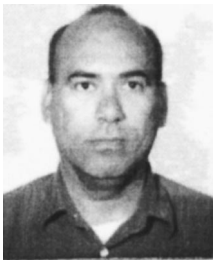
We can see similar results in Figs. 3(b) and 3(d), also in the green channel. The filter image [Fig. 3(h)] is a bacteria of different rotation. The peak is now at 90 deg because the bacteria is at 90 deg in orientation with respect to the test image.

These results show that it is possible to recognize the bacteria *Vibrio cholerae* O1 in the green channel irrespective of size, orientation, and position changes. Only *Vibrio cholerae* O1 can be recognized in the green channel. The presence of correlation peaks in the other two channels represents a false identification.

## References

1. R. R. Colwell, "Global climate and infectious disease: The cholera paradigm," *Science* **274**, 2025–2031 (1996).
2. R. R. Mouriño-Pérez, "Oceanography and the seventh cholera pandemic" *Epidemiology* **9**(3), 355–357 (1998).
3. K. Wachsmuth, G. K. Morris, and J. C. Feeley, "Vibrio," in *Manual of Clinical Microbiology*, 3rd ed., E. H. Kennette, A. Balows, W. J. Hausler, and J. P. Truant, Eds., pp. 226–234, American Society for Microbiology, Washington, DC (1980).
4. R. R. Colwell and A. Huq. "Vibrios in the environment: viable but nonculturable *Vibrio cholerae*," in *Vibrio Cholerae and Cholera: Molecular to Global Perspectives*, pp. 117–134, American Society for Microbiology, Washington, DC (1994).
5. H.-S. Xu, N. Roberts, L. Singleton, R. W. Attwell, D. J. Grimes, and R. R. Colwell, "Survival and viability of nonculturable *Escherichia coli* and *Vibrio cholerae* in the estuarine and marine environment," *Microb. Ecol.* **8**, 313–323 (1982).
6. Food and Drug Administration, *Bacteriological Analytical Manual*, 7th ed., AOAC International, Arlington VA (1992).
7. P. I. Fields, T. Popovic, K. Wachsmuth, and O. Olsvik, "Use of polymerase chain reaction for detection of toxigenic *Vibrio cholerae* O1 strains from the Latin american cholera epidemic," *J. Clin. Microbiol.* **30**(8), 2118–2121 (1992).
8. M. T. Suzaki, E. B. Shen, and B. F. Sherr, "DAPI direct counting underestimates bacterial abundances and average cell size compared to AO direct counting," *Limnol. Oceanogr.* **38**(7), 1566–1570 (1993).
9. J. P. Back and R. G. Kroll, "The differential fluorescence of bacteria stained with acridine orange and the effects of heat," *J. Appl. Bacteriol.* **71**, 51–58 (1991).
10. P. R. Brayton and R. R. Colwell, "Fluorescent antibody staining method for enumeration of viable environmental *Vibrio cholerae* O1," *J. Microbiol. Meth.* **6**, 309–314 (1987).
11. A. Huq, R. R. Colwell, R. Rahman, A. Ali, A. R. Chowdhury, S. Parveen, D. A. Sack, and E. Russek-Cohen, "Detection of *Vibrio cholerae* O1 in the aquatic environment by fluorescent-monoclonal antibody and culture methods," *Appl. Environ. Microbiol.* **56**(8), 2370–2373 (1990).
12. J. A. K. Hasan, D. Bernstein, A. Huq, L. Loomis, M. L. Tamplin, and R. R. Colwell, "Cholera DFA: an improved direct fluorescent monoclonal antibody staining kit for rapid detection and enumeration of *Vibrio cholerae* O1," *FEMS Microbiol. Lett.* **120**, 143–148 (1994).
13. A. VanderLugt, "Signal detection by complex spatial filter," *IEEE Trans. Inf. Theory* **IT-10**, 139–145 (1964).
14. V. A. Zavala-Hamz and J. Alvarez-Borrego, "Circular harmonic filters for the recognition of marine microorganisms," *Appl. Opt.* **36**, 484–489 (1997).
15. J. L. Pech-Pacheco and J. Alvarez-Borrego, "Optical-digital system applied to the identification of five phytoplankton species," *Mar. Biol. (Berlin)* **132**, 357–365 (1998).
16. M. S. Millán, J. Campos, C. Ferreira, and M. J. Yzuel, "Matched filter and phase only filter performance in colour image recognition," *Opt. Commun.* **73**(4), 277–284 (1989).
17. M. S. Millán, M. J. Yzuel, J. Campos, and C. Ferreira, "Strategies for the color character recognition by optical multichannel correlation," *Proc. SPIE* **1507**, 183–197 (1991).
18. M. S. Millán, N. Vila, and M. J. Yzuel, "Colour reversal films in multichannel optical correlators for olyphromatic image recognition," *Pure Appl. Opt.* **1**, 199–218 (1992).
19. V. Kober, V. Lashn, I. Moreno, and J. Campos, "Color component transformations for optical pattern recognition," *J. Opt. Soc. Am. A* **14**, 2656–2669 (1997).
20. P. Blake. "Historical perspectives on pandemic cholera," in *Vibrio cholerae and Cholera: Molecular to Global Perspectives*, pp. 293–295, American Society for Microbiology, Washington, DC (1994).

21. J. Fernández-de Castro, "El cólera: un problema no resuelto," *Ciencias* **24**, 33–44 (1991).
22. R. Tauxe, L. Seminario, R. Tapia, and M. Libel. "The Latin American epidemic," in *Vibrio cholerae and Cholera: Molecular to Global Perspectives*, pp. 321–345, American Society for Microbiology, Washington, DC (1994).
23. F. L. Singleton, R. Attwell, M. S. Jangi, and R. R. Colwell, "Effects of temperature and salinity on *Vibrio cholerae* growth," *Appl. Environ. Microbiol.* **44**, 1047–1058 (1982).
24. F. L. Singleton, R. Attwell, M. S. Jangi, and R. R. Colwell, "Influence of salinity and organic nutrients concentration on survival and growth of *Vibrio cholerae* in aquatic microcosms," *Appl. Environ. Microbiol.* **43**, 1080–1085 (1982).
25. M. L. Tamplin and R. R. Colwell, "Effects of microcosm salinity and organic substrate concentration on production of *Vibrio cholera* enterotoxin," *Appl. Environ. Microbiol.* **52**, 297–301 (1982).
26. J. Byrd, H.-S. Xu, and R. R. Colwell, "Viable but nonculturable bacteria in drinking water," *Appl. Environ. Microbiol.* **57**, 875–878 (1991).
27. D. Sharp and D. R. McLain, "Comments on the global ocean observing capabilities, indicator species as climate proxies, and the need for timely ocean monitoring," *Oceanography* **5**, 163–168 (1992).
28. K. H. Mann and J. R. N. Lazier, *Dynamics of Marine Ecosystems: Biological-Physical Interactions in the Oceans*, Blackwell Science, Cambridge, MA (1991).
29. P. R. Epstein, "Emerging diseases and ecosystems instability: new threats to public health," *Am. J. Public Health* **85**, 168–172 (1995).
30. J. Goodman, *Introduction to Fourier Optics*, McGraw-Hill, New York (1968).
31. G. Arfken, *Mathematical Methods for Physicists*, 3rd ed. Academic Press, Harcourt Brace Jovanovich, San Diego (1981).
32. L. Cohen, *Time-Frequency Analysis*, Prentice Hall Signal Processing Series, Upper Saddle River, NJ (1995).
33. J. A. Cuesta Merino, "Aplicación de la transformada de escala en el análisis de imágenes," Universidad Politécnica de Madrid, Escuela Técnica Superior de Ingenieros en Telecomunicación, Proyecto de fin de carrera (1999).
34. D. Casasent and D. Psaltis, "Scale invariant optical transform," *Opt. Eng.* **15**(3), 258–261 (1976).
35. J. L. Pech-Pacheco, G. Cristóbal, J. Alvarez-Borrego, and M. Keil, "Automatic object identification irrespective to geometric changes," *Opt. Eng.* submitted for publication.
36. J. Campos, M. S. Millan, M. J. Yzuel, and C. Ferreira, "Color invariant character recognition and character-background color identification by multichannel matched filter," *Proc. SPIE* **1564**, 189–198 (1991).



**Josué Alvarez-Borrego** received his BS degree in physical oceanography in 1980 from the Facultad de Ciencias Marinas, Ensenada, B. C., Mexico, and his MSc and PhD degrees in optics in 1983 and 1993 from CICESE, Mexico. Currently he is a titular researcher with the Optics Department, CICESE, Mexico. His research interests are image processing with applications to biogenic particles and image processing of the sea surface. Dr. Alvarez-

Borrego has directed several theses, has published more than 25

papers in international journals, and has presented more than 70 works at national and international congresses. He is a member of the Mexican Academy of Optics, Researches National System (SNI), and the Sciences Mexican Academy.



**Rosa Reyna Mouriño-Pérez** received her MD degree from UAM-Xochimilco in 1985, her MS degree in research in public health from UAM-Iztapalapa in 1989, and her PhD in marine ecology from CICESE in 1999. She is currently a posdoctoral fellow in marine microbiology at Scripps Institute of Oceanography UCSD. She was a professor with the School of Medicine, UNAM, from 1988 to 1996 and a professor with the Marine Sciences Faculty, UABC, from 1997 to 1999. She has published more than 15 papers in national and international journals and 4 book chapters, and has presented more than 25 works at national and international congresses. She has been a member of the Mexican Society of Public Health since 1988, the Mexican Society of Cardiology since 1995, and the Mexican Association for the Prevention of Atherosclerosis and Its Complications since 1995.



**Gabriel Cristóbal-Pérez** received his MSc and PhD degrees in electrical engineering from the Universidad Politécnica de Madrid in 1979 and 1986, respectively. He has held visiting appointments at the International Computer Science Institute in 1989 to 1991 and at the Electronics Research Lab, University of California, Berkeley, in 1991. He joined the Instituto de Optica (CSIC) in 1993, where he held a tenured scientist position. He has published a number of papers in the area of time-frequency representations and texture and pattern analysis. He is a fellow of the IEEE.



**José Luis Pech-Pacheco** is currently a posdoc with the Department of Image and Vision, Institute of Optic at Consejo Superior de Investigación Científica, Spain, working under the guidance of Dr. Gabriel Cristóbal in the areas of image processing, automatic system identification of diatoms, automatic microscopic systems, medical imaging, security systems, and optical-digital pattern recognition. Dr. Pech received his BSc degree from the Facultad de Ciencias Marinas at UABC, México, in 1993, followed by his MS Honors degree in the areas of oceanography in 1995, and his PhD degree from CICESE, Mexico, in the area of ecology marine.